

Observation of Laser-Assisted Electron-Atom Scattering in Femtosecond Intense Laser Fields

Reika Kanya,¹ Yuya Morimoto,¹ and Kaoru Yamanouchi^{1,2,*}

¹Department of Chemistry, School of Science, The University of Tokyo, 7-3-1 Hongo, Bunkyo-ku, Tokyo 113-0033, Japan

²NANOQUINE, The University of Tokyo, 7-3-1 Hongo, Bunkyo-ku, Tokyo 113-0033, Japan

(Received 19 July 2010; published 13 September 2010)

Laser-assisted electron scattering (LAES) in a femtosecond near-infrared intense laser field was observed through the scattering of 1 keV electrons by xenon atoms. The intensities, angular distributions, and laser polarization dependence of the observed LAES signals for the energy gain ($+\hbar\omega$) and energy loss ($-\hbar\omega$) processes were interpreted well by numerical simulations. As an application of this femtosecond-LAES process, a new method of time-resolved gas electron diffraction for probing geometrical change of molecules with high precision is proposed.

DOI: 10.1103/PhysRevLett.105.123202

PACS numbers: 34.80.Qb

When an electron collides with an atom in a laser field, the electron can gain or lose its energy through the scattering process by a unit of the photon energy. This process of energy gain or energy loss of $n\hbar\omega$ (n : integer) is called laser-assisted electron scattering (LAES) [1,2]. The observation of the $\pm\hbar\omega$ energy shifts in electron-atom elastic scattering processes was reported first by Andrick and Langhans with a cw-CO₂ laser in 1976 [3]. Next year, Weingartshofer *et al.* reported multiphoton energy gain and energy loss in an electron-argon collision in a laser field generated by a pulsed CO₂ laser [4]. Since then, cw- and pulsed-CO₂ lasers have been employed in the LAES experiments, where the laser fields were in a rather moderate intensity range ($< 10^9$ W/cm²), in the midinfrared region ($\lambda = 10.6$ μ m), and with the minimum pulse duration of the order of microseconds [1]. In most cases, the experimental data were in reasonable agreement with the predictions of the Kroll-Watson theory [5], which is formulated under the following three assumptions; (i) laser-target interaction is negligibly small, (ii) photon energy is much smaller than kinetic energy of incident electrons, (iii) scattering is nonresonant in the absence of a laser field.

When the laser-atom interaction becomes large in intense laser fields, the Kroll-Watson theory is not an appropriate approximation of the LAES process. Then, an effect of the formation of light-dressed atoms, which are created through an electronic-state mixing by the laser-atom interaction, becomes significant in the LAES process. Byron and Joachain theoretically investigated this situation by treating the laser-atom interaction as the first-order time-dependent perturbation [6], while treating the electron-atom interaction by the first-order Born approximation. Nonperturbative interaction between a laser field and an atom in a process of high-energy electron-atom scattering were treated by Born-Floquet theory proposed by Faisal [7], and by non-Hermitian Born-Floquet theory developed by Dörr *et al.* [8]. These studies reported that a pronounced peak structure at the zero scattering angle ($\theta = 0$ degree)

appears in the differential cross section of the LAES by light-dressed atoms [6], and the peak intensity increases significantly through the resonant interaction between atoms and the laser field [8]. Therefore, LAES experiments under the strong laser-atom interaction will give us valuable information on light-dressed states of atoms in intense laser fields. However, in the previous LAES experiments [1] with the moderate field intensities in the midinfrared region, where the photon energy is far from resonance energies of electronic transitions of target atoms, the effect of the laser-atom interaction on the differential cross section was negligibly small, as concluded by several theoretical estimations [9–11].

Nowadays, an intense laser field over 10^{12} W/cm² in the near-infrared region (~ 800 nm) can be achieved easily by femtosecond Ti:sapphire lasers, where the light-dressed atoms can securely be created. However, the LAES signals in femtosecond laser fields are estimated to be extremely weak because the signal intensity of LAES is proportional to the interaction time with the laser fields, as long as the laser field intensity and the wavelength are constant. For example, the LAES signal intensity with a 200 fs pulse is only 10^{-7} relative to that with a 2 μ s pulse, that is a typical pulse duration employed in the previous study [4]. Therefore, an experimental demonstration of the LAES with femtosecond near-infrared intense laser pulses should be a challenging step for investigations of the LAES phenomena. The present study demonstrates a LAES experiment under such laser field conditions (1.8×10^{12} W/cm², 795 nm, 200 fs) for the first time.

The femtosecond-LAES apparatus consists of an electron beam source, a scattering chamber, a toroidal-type electron energy analyzer, and an imaging detector (Fig. 1). The output of a 5 kHz Ti:sapphire laser system ($\lambda = 795$ nm, 0.8 mJ/pulse, $\Delta t = 200$ fs, linearly polarized) is introduced into the scattering point through a combination of a cylindrical lens ($f = 10$ m) and a spherical lens ($f = 400$ mm), so that the laser beam profile at the scattering point takes an elliptical shape which ensures a

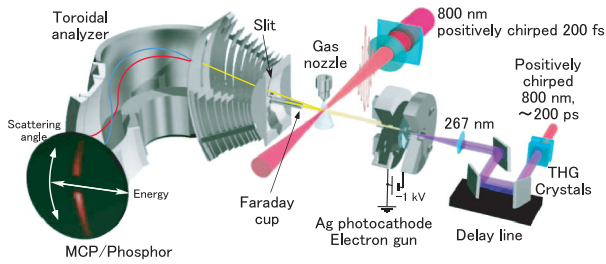


FIG. 1 (color). The schematic of the experimental setup.

maximum spatial overlap between three beams, that is, an atomic beam, an electron beam, and the laser beam. The peak laser field intensity is estimated to be 1.8×10^{12} W/cm² at the scattering point. The 200 fs laser pulses are obtained by chirping positively transform-limited 50 fs pulses.

A pulsed electron beam is created at a surface of a silver-coated photocathode through the photoelectric effect by irradiating the surface with UV laser pulses ($\lambda = 267$ nm), which are generated as THG of chirped fundamental pulses that are partially split from the main pulses before a pulse compressor of the laser system. The generated electron packets are accelerated to 1 keV within a 0.3 mm distance between the cathode and a grounded anode, and collimated by an electromagnetic lens and a series of pinholes. A laser-electron synchronization and the measurement of the electron pulse duration were achieved by the electron shadowgraph technique proposed by Park *et al.* [12] in their pulsed electron diffraction experiment. The electron pulse duration was determined to be 45 ± 5 ps.

The collimated electron pulse intersects the xenon gas flow and laser beam at right angles in the scattering chamber. The scattered electrons are introduced into the electron energy analyzer through a 0.8 mm slit. The direction of the slit is set to be vertical (Fig. 1). Unscattered electrons and scattered electrons within a small angle ($\theta < 2$ degree) are blocked by a Faraday cup located in front of the entrance slit of the analyzer. The kinetic energy and angular distributions of the scattered electrons passing through the energy analyzer are recorded as the 2D image on a gated-microchannel plate (MCP) equipped with a phosphor screen coupled with a CCD camera. After every one-second exposure with the camera, electron signals are detected by a counting method. The averaged count rate of the electron signals was around 10 cps, i.e., 2×10^{-3} counts per shot at the 5 kHz repetition rate. For securing that the experimental conditions are kept constant all the time during the long time accumulation, the experimental conditions were checked every six hours and slightly adjusted, if necessary. It was confirmed from the elastic scattering experiment of a Xe gas that the energy resolution of 0.7 eV was achieved, which is sufficiently high for observing the LAES phenomena because the LAES signals appear with the energy interval of 1.56 eV corresponding to the one-photon energy of the laser light.

The obtained raw images of scattered electrons are shown in Fig. 2. Figure 2(a) shows electron scattering signals when the laser pulse was introduced at the instance of the electron scattering by Xe atoms. The laser polarization was set to be “vertical”, i.e., perpendicular to the electron beam axis (Fig. 1). Figure 2(b) shows background signals, which was obtained when the temporal delay of the electron pulse with respect to the laser pulse was set to be +100 ps. The net exposure time was around 83 hours for both images. The intense patterns of arcuate lines seen at the central area of both images are the elastic scattering signals. As indicated by the white arrows in Fig. 2(a), the weak patterns of arcuate lines can be seen on both sides of the central arcuate line, while such side-structures could not be seen in Fig. 2(b).

The observed difference in Fig. 2 becomes clearer when the electron energy spectra were obtained through the integration of the 2D signals over the scattering angles along the arcuate isoenergetic coordinate. In the integration, signals in the region of $y > 105$ pixel in Fig. 2 were excluded from the analysis because the contributions of stray electrons are significantly large in the region. The red filled circles plotted in Fig. 3(a) show the energy spectrum of the electrons scattered in the laser field, and the black filled circles correspond to the background signals. Small but unambiguous increases in the signal intensity appear at the kinetic-energy shifts of $\pm\hbar\omega$, i.e., ± 1.56 eV, in Fig. 3(a) (red filled circles). The red filled circles in Fig. 3(b) represent the LAES signals obtained through subtraction of the background signals from the scattering signals in the laser field in Fig. 3(a). Both of the signals at the energies of $\pm\hbar\omega$ can be recognized as distinct peak structures with similar peak intensities of 3×10^{-4} relative to the elastic scattering intensity. This is clear experimental confirmation that the $n = \pm 1$ transitions in the LAES process were observed. Furthermore, slight increases in the signal intensities at the energy shifts of $\pm 2\hbar\omega$, approximately, can be recognized, possibly representing the two-photon LAES transitions.

In order to secure our assignment, the relative intensities of the LAES signals were estimated by a numerical

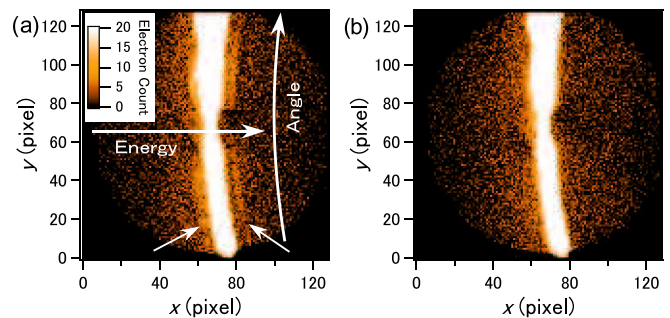


FIG. 2 (color online). The raw images of (a) scattered electrons with vertically polarized laser fields, and (b) background signals.

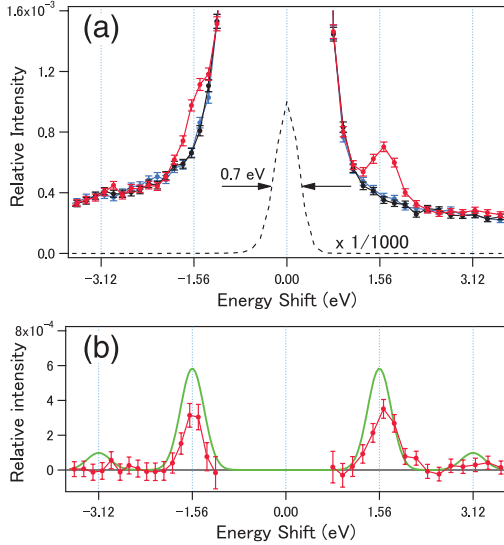


FIG. 3 (color). The energy spectra of relative intensities of scattered electron signals. Each relative intensity is normalized by the peak intensity of the elastic signal. Estimated statistical error bars are derived from square roots of signal counts. (a) Red (blue) filled circles: Electron signals with vertically (horizontally) polarized laser fields. Black filled circles: Background signals. Broken line: A elastic peak reduced by a factor of 1000. (b) Red filled circles: A subtraction of the backgrounds from the signals with vertically polarized laser fields. Green line: A calculated spectrum.

simulation. Since the high-energy electron beam with 1 keV incident energy was employed in the present experiment, LAES cross sections can be calculated with the Bunkin-Fedorov approximation (BFA) [13], where the electron-atom interaction is treated within the first Born approximation. In the BFA, the differential cross section for net n -photon absorption, $d\sigma_{\text{BFA}}^{(n)}/d\Omega$, is represented as

$$\frac{d\sigma_{\text{BFA}}^{(n)}}{d\Omega} = \frac{|\mathbf{p}_f|}{|\mathbf{p}_i|} J_n^2\left(\frac{e}{m\omega^2} \boldsymbol{\varepsilon} \cdot \mathbf{s}\right) \frac{d\sigma_{\text{el}}}{d\Omega}, \quad (1)$$

where $J_n(x)$ is the n th order Bessel function of the first kind, \mathbf{p}_i and \mathbf{p}_f are initial and final electron momenta, e is unit charge, $\boldsymbol{\varepsilon}$ is an electric amplitude vector of the laser field, m is mass of an electron, \mathbf{s} is a scattering vector defined by $(\mathbf{p}_f - \mathbf{p}_i)/\hbar$, and $d\sigma_{\text{el}}/d\Omega$ is a differential cross section of elastic scattering without laser fields. Considering the spatial profile of the three beams and the temporal envelopes of the laser pulse and the electron pulse, the spatiotemporal averaging of Eq. (1) under the present experimental conditions was performed in the simulation. The result of the simulation is plotted by the green solid line in Fig. 3(b). The relative intensities derived from the simulation are in good agreement with those in the experimental results.

When the laser polarization vector is set to be ‘‘horizontal’’, i.e., parallel to the direction of the incident electron

beam (Fig. 1), the polarization vector becomes nearly perpendicular to the scattering vector, \mathbf{s} , for the forward scattering of high-energy electrons. Then, the LAES signal intensities except at $n = 0$ should be suppressed significantly because the argument of the Bessel function in Eq. (1) becomes nearly zero. This significant polarization dependence should provide a further verification for our assignment. In Fig. 3(a), an energy spectrum with the horizontally polarized laser fields is plotted by the blue filled circles. In contrast to the vertically polarized case, no distinguishable difference from the backgrounds (black filled circles) was observed. This result is consistent with the corresponding numerical calculation, which yielded a relative intensity of 7×10^{-6} for $n = \pm 1$ transitions.

Figure 4 shows the angular distributions of the LAES signals with the vertically polarized laser field for $n = +1$ (black filled circles) and $n = -1$ (red filled circles) transitions, which were obtained by the subtraction of the background signal. The green solid line is a result of the numerical calculation considering the angular dependence of the detection efficiency, which was estimated from the angular dependence of the elastic signal intensity. The calculated angular distribution is in good agreement with the experimental results.

When the presently demonstrated femtosecond-LAES is applied to molecular samples, instantaneous molecular structure can be determined with femtosecond temporal resolution, as demonstrated through the following model calculation. Figure 5(a) shows the results of numerical calculations of the scattering intensities as a function of $s = |\mathbf{s}|$ for the $n = +1$ transition of LAES by Cl_2 molecules with the three different internuclear distances; 2.0, 3.0, and 4.0 Å. The properties of the three beams and their spatiotemporal overlap were assumed to be the same as the present experimental condition. Through the same procedure as in the conventional gas electron diffraction method [14,15], a modified molecular scattering intensity, $sM(s)$, was obtained from the angular distribution [Fig. 5(b)]. Then, a radial distribution function of internuclear distances, $D(r)$, can be derived through the Fourier

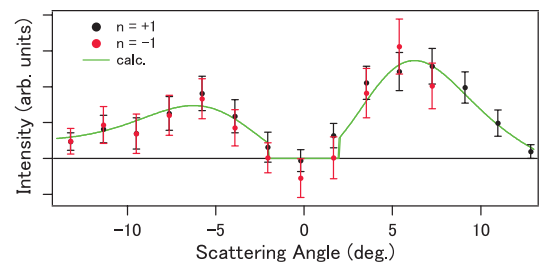


FIG. 4 (color). The angular distributions of LAES for the $n = \pm 1$ transitions with the vertically polarized laser field. Black (red) filled circles: Observed LAES signals of $n = +1$ ($n = -1$). Green line: numerical calculation. Because of the large contribution of stray electrons, data at $\theta > 10$ degree were excluded from the analysis for the $n = -1$ transition.

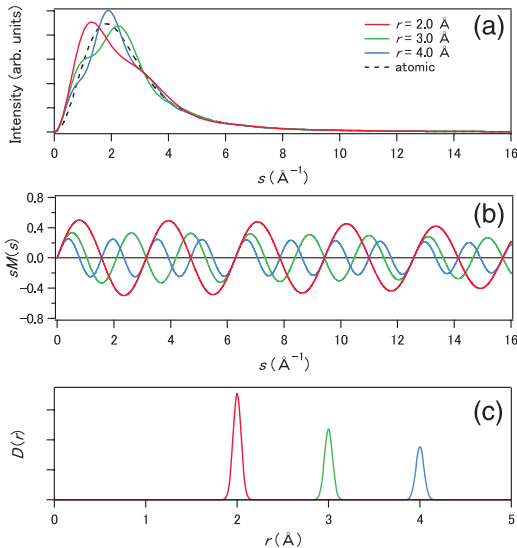


FIG. 5 (color). The model calculations of (a) scattering intensities, (b) $sM(s)$, and (c) $D(r)$ of LAES by Cl_2 molecule with the different internuclear distances; $r = 2.0 \text{ \AA}$ (red line), 3.0 \AA (green line), and 4.0 \AA (blue line) for the $n = +1$ transition. The mean amplitude of r is set to be 0.044 \AA . Broken line in (a): the atomic scattering intensity.

transformation of $sM(s)$ [Fig. 5(c)]. Considering the fact that LAES signals arise only when molecules are interacting with an ultrashort laser field, the determined molecular structure is “an instantaneous structure” during the femtosecond laser pulse duration. Therefore, if dynamical molecular processes initiated by femtosecond pump laser pulses are proved by the femtosecond LAES, the temporal resolution of the gas electron diffraction will be of the order of femtoseconds, i.e., 10^2 – 10^3 times better than $\sim 1 \text{ ps}$ achieved by the previous pulsed gas electron diffraction methods [16]. Similarly to the conventional gas electron diffraction experiments [14], LAES experiments with higher kinetic-energy electrons (the order of 10^4 eV) will provide internuclear distances with a high precision better than $\pm 0.01 \text{ \AA}$. It may be true that some structural information of molecules can be extracted from a diffraction method using a recolliding electron packet as an incident electron beam [17,18], but instantaneous geometrical structures of molecules with high precision can unambiguously be determined with femtosecond temporal resolution by the presently proposed LAES approach.

In the present study, the LAES in intense femtosecond laser fields was observed for the first time. Compared to the previous LAES experiments [1], the laser field intensity was increased by a factor of 10^3 , and the laser pulse

duration was shortened by a factor of 10^{-7} . As an application of the femtosecond-LAES, a new electron diffraction technique with femtosecond temporal resolution was proposed through the model calculations of the LAES by Cl_2 molecules.

We gratefully acknowledge helpful discussions with F.H.M. Faisal. The research was supported by the Grant-in-Aid for Specially Promoted Research (Grant No. 19002006), the Grant-in-Aid for Young Scientists (B) (Grant No. 19750003), Global COE Program (Chemistry Innovation through Cooperation of Science and Engineering), and Special Coordination Funds for Promoting Science and Technology, from Ministry of Education, Culture, Sports, Science and Technology (MEXT), Japan.

*kaoru@chem.s.u-tokyo.ac.jp

- [1] N. J. Mason, *Rep. Prog. Phys.* **56**, 1275 (1993).
- [2] F. Ehlötzky, A. Jaroń, and J. Z. Kamiński, *Phys. Rep.* **297**, 63 (1998).
- [3] D. Andrick and L. Langhans, *J. Phys. B* **9**, L459 (1976).
- [4] A. Weingartshofer, J. K. Holmes, G. Caudle, E. M. Clarke, and H. Krüger, *Phys. Rev. Lett.* **39**, 269 (1977).
- [5] N. M. Kroll and K. M. Watson, *Phys. Rev. A* **8**, 804 (1973).
- [6] F. W. Byron, Jr., and C. J. Joachain, *J. Phys. B* **17**, L295 (1984).
- [7] F. H. M. Faisal, *Theory of Multiphoton Processes* (Plenum, New York, 1987) Section 12.3.4.
- [8] M. Dörr, C. J. Joachain, R. M. Potvliege, and S. Vučić, *Phys. Rev. A* **49**, 4852 (1994).
- [9] I. Rabadán, L. Méndez, and A. S. Dickinson, *J. Phys. B* **27**, L535 (1994).
- [10] S. Geltman, *Phys. Rev. A* **51**, R34 (1995).
- [11] S. Varró and F. Ehlötzky, *Phys. Lett. A* **203**, 203 (1995).
- [12] H. Park, Z. Hao, X. Wang, S. Nie, R. Clinite, and J. Cao, *Rev. Sci. Instrum.* **76**, 083905 (2005).
- [13] F. V. Bunkin and M. V. Fedorov, *Sov. Phys. JETP* **22**, 844 (1966).
- [14] K. Yamanouchi, M. Sugie, H. Takeo, C. Matsumura, and K. Kuchitsu, *J. Phys. Chem.* **88**, 2315 (1984).
- [15] *Stereochemical Applications of Gas-Phase Electron Diffraction, Part A*, edited by I. Hargittai and M. Hargittai (Wiley-VCH Verlag GmbH, New York, 1988).
- [16] R. Srinivasan, V. A. Lobastov, C. Ruan, and A. H. Zewail, *Helv. Chim. Acta* **86**, 1761 (2003).
- [17] T. Zuo, A. D. Bandrauk, and P. B. Corkum, *Chem. Phys. Lett.* **259**, 313 (1996).
- [18] M. Meckel, D. Comtois, D. Zeidler, A. Staudte, D. Pavičić, H. C. Bandulet, H. Pépin, J. C. Kieffer, R. Dörner, D. M. Villeneuve, and P. B. Corkum, *Science* **320**, 1478 (2008).